HHS Public Access

Author manuscript

Eur J Heart Fail. Author manuscript; available in PMC 2018 December 01.

Published in final edited form as:

Eur J Heart Fail. 2017 December ; 19(12): 1675–1685. doi:10.1002/ejhf.913.

Physiologic dead space and arterial carbon dioxide contributions to exercise ventilatory inefficiency in patients with reduced or preserved ejection heart failure

Erik H. Van Iterson[1], **Bruce D. Johnson**[1], **Barry A. Borlaug**[1], and **Thomas P. Olson**[1]

[1]Department of Cardiovascular Medicine, Mayo Clinic, Rochester MN

Abstract

Aims—Patients with heart failure (HF) with reduced (HFrEF) or preserved (HFpEF) ejection fraction demonstrate an increased ventilatory equivalent for carbon dioxide ($\dot{V}_E/\dot{V}CO_2$) slope. The physiologic correlates of $\dot{V}_E/\dot{V}CO_2$ slope remain unclear in the two HF phenotypes. We hypothesized that changes in physiologic dead space to tidal volume ratio (V_D/V_T) and arterial CO_2 tension ($PaCO_2$) differentially contribute to $\dot{V}_E/\dot{V}CO_2$ slope in HFrEF versus HFpEF.

Methods and Results—Adults with HFrEF (N=32) and HFpEF (N=27) (LVEF: 22±7 and 61±9%; BMI: 28±4 and 33±6 kg/m^2, P<0.01) performed cardiopulmonary exercise testing with breath-by-breath ventilation and gas-exchange measurements. $PaCO_2$ was measured via radial arterial catheterization. We calculated $\dot{V}_E/\dot{V}CO_2$ slope via linear regression, and $V_D/V_T=1-[(863\times\dot{V}CO_2)/(\dot{V}_E\times PaCO_2)]$. Resting V_D/V_T (0.48±0.08 vs. 0.41±0.11, P=0.04), but not $PaCO_2$ (38±5 vs. 40±3 mm Hg, P=0.21) differed in HFrEF versus HFpEF, respectively. Peak exercise V_D/V_T (0.39±0.08 vs. 0.32±0.12, P=0.02) and $PaCO_2$ (33±6 vs. 38±4 mm Hg, P<0.01) differed in HFrEF versus HFpEF, respectively. $\dot{V}_E/\dot{V}CO_2$ slope was higher in HFrEF compared to HFpEF (44±11 vs 35±8, P<0.01). Variance associated with $\dot{V}_E/\dot{V}CO_2$ slope in HFrEF and HFpEF was explained by peak exercise V_D/V_T (R^2=0.30 vs. 0.50, respectively) and $PaCO_2$ (R^2=0.64 vs. 0.28, respectively), but with different relative contributions from each (all P<0.01).

Conclusions—Relationships between $\dot{V}_E/\dot{V}CO_2$ slope with both V_D/V_T and $PaCO_2$ are robust, but differ in HFpEF compared to HFrEF. Increasing $\dot{V}_E/\dot{V}CO_2$ slope appears strongly explained by mechanisms influential to regulating $PaCO_2$ in HFrEF, which contrasts the strong role of increased V_D/V_T in HFpEF.

Correspondence and Reprint Requests to: Erik H. Van Iterson, PhD, MS, MA, Department of Cardiovascular Medicine, Mayo Clinic, 200 First St SW, Rochester, MN 55905, vaniterson.erik@mayo.edu, Phone: 773-433-0787, Fax: 507-255-4861.

All aspects of the work in this manuscript were performed at Mayo Clinic, Rochester MN

Positions, institution, and location of authors:

Erik H. Van Iterson, PhD: Research Fellow in Cardiovascular Medicine, Mayo Clinic, Rochester MN

Bruce D. Johnson, PhD: Professor of Medicine and Professor of Physiology, Mayo Clinic, Rochester MN

Barry A. Borlaug, MD: Associate Professor of Medicine, Mayo Clinic, Rochester MN

Thomas P. Olson, PhD: Associate Professor of Medicine, Mayo Clinic, Rochester MN

Conflicts of Interest: none declared.

Keywords

Cardiopulmonary exercise testing; exercise ventilatory efficiency; exercise capacity; exercise tolerance; exercise intolerance; HFpEF

Introduction

A steep slope of the ventilatory equivalent for carbon dioxide ($\dot{V}_E/\dot{V}CO_2$) as quantified during cardiopulmonary exercise testing (CPET) demonstrates robust prognostic power in heart failure (HF) patients with reduced (HFrEF) or preserved (HFpEF) ejection fraction (1–4). Ventilatory inefficiency is suggested to accompany an excessive rate-mediated rise in $\dot{V}_E/\dot{V}CO_2$ slope, which is likely both a consequence and key contributor to exercise intolerance in HF (2–5). In this context, despite the broad clinical and research use of $\dot{V}_E/\dot{V}CO_2$ slope to phenotype the magnitude of exercise ventilatory inefficiency in HF, the understanding of this index has not been clearly defined in patients with HFrEF or HFpEF.

The $\dot{V}_E/\dot{V}CO_2$ slope is determined by dynamic coupling of gas exchange and hemodynamics reflecting pulmonary, cardiac, musculoskeletal, and nervous system responses to exercise (4, 6–8). 'Ideal' alveolar gas and air equations implicate the proportion of tidal volume distributed to physiologic dead space (V_D/V_T) accompanied by mechanisms underpinning regulation of arterial carbon dioxide tension ($PaCO_2$) as key contributors to $\dot{V}_E/\dot{V}CO_2$ slope (4, 6, 7, 9). While increased $\dot{V}_E/\dot{V}CO_2$ slope is likely to be the consequence of integrated factors including wasted alveolar ventilation ($\dot{V}_A$), atelectasis, and/or impaired neural ventilatory control, there is controversy as to which event is the principal mediator in HFrEF (4, 7, 9, 10), with even less information available on this topic in HFpEF. Further complicating this discussion is the evolving knowledge of what unique characteristics unequivocally define the HFpEF phenotype (2, 3, 5, 11, 12).

Guazzi et al. (4) demonstrated that high $\dot{V}_E/\dot{V}CO_2$ slope from rest to peak exercise is predictive of survival in HFrEF. Similar to data from Woods et al. (7) during submaximal exercise, Guazzi et al. (4) attributed increased $\dot{V}_E/\dot{V}CO_2$ slope to influences of impaired mechanisms of ventilatory control (e.g., low $PaCO_2$ regulatory set-points) accompanied by contributions from elevated V_D/V_T. By contrast, without observations from specific tests of ventilatory control, Sullivan et al. (9) and others (10) suggest that ventilatory control related to regulation of $PaCO_2$ is intact in HFrEF, whereas abnormal physiologic hemodynamic factors are more likely present in this population.

As a necessary hypothesis-generating step towards advancing the understanding and interpretation of $\dot{V}_E/\dot{V}CO_2$ slope in HF, this study aimed to demonstrate how $\dot{V}_E/\dot{V}CO_2$ slope is related to changes in V_D/V_T and $PaCO_2$ during CPET in patients with HFrEF or HFpEF. We hypothesized that increased V_D/V_T accompanied by decreased $PaCO_2$ would differentially explain the rise in $\dot{V}_E/\dot{V}CO_2$ slope in HFrEF compared to HFpEF.

Methods

Participants

Patients with HFrEF or HFpEF (N=59) were referred by their primary cardiologist for CPET as part of a comprehensive HF evaluation at Mayo Clinic, Rochester, MN. Using the European Society of Cardiology criteria, we studied 32 HFrEF (left ventricular ejection fraction [LVEF] ≤40%) and 27 HFpEF (LVEF >50%) (Characteristics, Table 1) (13).

Patients were excluded based on the following criteria: significant coronary artery disease (stenosis ≥50%), cor pulmonale, diagnosed pulmonary disease secondary to HF, primary renal or hepatic disease, valvular heart disease (any stenosis, >mild regurgitation, etc.), hypertrophic or infiltrative cardiomyopathy, constrictive pericarditis, or deep vein thrombosis. All aspects of this study were approved by the Mayo Clinic Institutional Review Board while conforming to principles outlined in the Declaration of Helsinki. All authors have read and agreed to the manuscript as written.

Echocardiography

Resting two-dimensional and tissue Doppler echocardiography according to guidelines of the American Society of Echocardiography were used to assess LVEF, morphology, and function; as well as early transmitral flow velocity (E), late transmitral flow velocity (A), E/A ratio, early diastolic mitral annular velocity (e′), peak E to e′ ratio, and left atrial volumes (Table 1) (13).

CPET protocol

Patients performed CPET in the morning in a fasted state while remaining on standard pharmacologic therapy. Patients exercised in a semi-recumbent position at an initial workload of 20-watts (W) while pedaling at 60–65 rpm, thereafter increasing by 10-W every 3 min until volitional fatigue. Heart rate and rhythm were continuously monitored using a 12-lead electrocardiogram.

Ventilation and gas exchange

Breath-by-breath open-circuit spirometry (CPX/D, MGC Diagnostics, St.Paul, MN) was used to continuously collect ventilation and gas exchange data throughout CPET. The final 30-s of rest and the final completed stage (i.e., peak pulmonary oxygen uptake, $\dot{V}O_{2peak}$) were used for data analyses. Data were acquired for variables: $\dot{V}O_2$, $\dot{V}CO_2$, respiratory exchange ratio (RER), respiratory rate (f_B), V_T, $\dot{V}_E$, end-tidal CO_2 tension ($P_{ET}CO_2$), and end-tidal O_2 tension ($P_{ET}O_2$). Percent (%) of predicted $\dot{V}O_{2peak}$ was calculated from Hansen et al. (14).

Arterial gas measurement and parameters

Continuous monitoring and periodic sampling of arterial blood gases occurred using standard technique via percutaneous insertion of a 20-gauge catheter at the left radial artery. Arterialized blood drawn into heparinized 3-mL glass syringes occurred so as to approximately align with breath-by-breath periods (i.e., final ~30-s of each CPET stage), with the final draw of the last completed stage used to describe peak exercise. Arterialized

samples were chilled on ice and immediately sent to our institutional core laboratory where standard processing techniques occurred for: $PaCO_2$, oxygen tension (PaO_2), pH (pHa), and oxygen saturation (SaO_2). From these measurements, we used standard physiologic and blood biochemical equations (described in Appendix) to derive bicarbonate (HCO_3^-) and base excess (BE) of arterialized blood.

Derived ventilation and gas exchange parameters

By using arterialized gas measurements combined with acquired basic ventilatory and gas exchange responses, 'ideal' alveolar gas and air equations with associated parameters were used to calculate: $\dot{V}_A$, alveolar volume (V_A), alveolar CO_2 tension ($PACO_2$), alveolar O_2 tension (PAO_2), alveolar-to-arterial O_2 difference ($PA\text{-}aO_2$), indirect simplified estimate of whole lung diffusing capacity for O_2 (DLO_2) via Fick's law of diffusion, and V_D ventilation ($\dot{V}_D$) (described in Appendix), whereas V_D/V_T equaled (4, 6–10),

$$\frac{V_D}{V_T} = \left(1 - \frac{863 \times \dot{V}\,CO_2}{\dot{V}_E \times PaCO_2}\right)$$

where 863 converts gas concentration to partial pressure while correcting for the fact that $\dot{V}CO_2$ is expressed as a dry gas volume at standard temperature (0°C), pressure (760 mm Hg), and dry (0% water vapor) (STPD), whereas ventilation is expressed as a wet gas volume at body temperature, pressure, and saturation (BTPS).

Mixed-expired CO_2 ($PECO_2$) equaled the quotient of 863 and $\dot{V}_E/\dot{V}CO_2$ (15). All data from rest to peak exercise was used to calculate $\dot{V}_E/\dot{V}CO_2$ slope via linear regression, which provided optimal data interpretability and temporal consistency across participants (16).

Statistical Analyses

Parametric data are presented as mean±SD. Results of Shapiro-Wilk and Levene's tests did not suggest data were significantly skewed or variance was heterogeneous. Between group baseline differences were compared using independent Student's t-tests for parametric data or χ^2-tests for categorical variables. Repeated measures ANOVA models with group-by-time interaction terms were used to test between-within group differences at rest and peak exercise. When *F*-tests from group-by-time interaction terms were significant, post-hoc Tukey-Kramer tests were used to assess between-within pairwise differences.

Ordinary least squares univariate linear regressions were used to test relationships between dependent (ordinate, $\dot{V}_E/\dot{V}CO_2$ slope) and independent (abscissa, V_D/V_T, $PaCO_2$, etc.) variables. Coefficient of determination (R^2) and regression equations, $y_{est} = a+bx$, were computed from these models. Interpretation of R^2 were based on standards of *Cohen* (17): modest=0.02; moderate=0.15; or strong≥0.25. Two-tailed significance was determined using an alpha level set at 0.05. Statistical analyses were performed using SAS statistical software v.9.4 (SAS Institute, Cary, NC).

Results

Participant characteristics

Both HFrEF and HFpEF demonstrated age, sex distribution, and LVEF consistent with currently recognized clinical phenotypes (Table 1). Despite greater %predicted $\dot{V}O_{2peak}$ in HFpEF versus HFrEF, there were no differences in $\dot{V}O_{2peak}$ (mL/kg/min). New York Heart Association and Weber-Janicki functional classifications aligned in HFpEF, but to a lesser extent in HFrEF. Compared to HFpEF, Hb was higher in HFrEF whereas creatinine and eGFR were similar. Frequency of therapies including ACE inhibitors, β-blockers (HFrEF, 6 and 22 on non-selective and β_1-selective, respectively; HFpEF, 17/17 on β_1-selective), digoxin, and diuretics were higher in HFrEF versus HFpEF. Resting echocardiography indicated there were increased LV filling pressures in HFrEF and HFpEF. Participants completed all aspects of this study in the absence of demonstrating adverse events (e.g., no signs/symptoms of pulmonary embolism, which could contribute to impaired ventilatory function).

Workload and basic ventilation and gas exchange

Resting $\dot{V}O_2$, $\dot{V}CO_2$, RER, $\dot{V}_E$, RR, V_T, $P_{ET}O_2$, and $PECO_2/P_{ET}CO_2$ were similar between groups, whereas $P_{ET}CO_2$ and $PECO_2$ were lower in HFrEF versus HFpEF (Table 2). Despite no differences in peak W and RER, HFrEF demonstrated lower $\dot{V}O_2$ and $\dot{V}CO_2$ versus HFpEF, whereas differences in $\dot{V}_E/\dot{V}CO_2$, $P_{ET}CO_2$, and $PECO_2$ persisted from rest. Except for $\dot{V}_E/\dot{V}CO_2$ (↓HFpEF), $P_{ET}CO_2$ (↓HFrEF), and $PECO_2$ (↑HFpEF), changes in other metrics from rest to peak exercise within HFrEF and HFpEF were similar (Table 2).

Alveolar equation and blood biochemistry parameters

Excluding lower resting V_D/V_T in HFpEF versus HFrEF (Figure 1), parameters associated with alveolar equations or blood biochemistry were similar between groups (Table 3). By contrast, consistent with higher $\dot{V}_E/\dot{V}CO_2$ slope in HFrEF (Figure 1A), HFrEF demonstrated higher V_D, $\dot{V}_D$, and V_D/V_T (Figure 1B) as well as lower $PaCO_2$ (Figure 1C) and $PACO_2$ accompanied by higher pHa versus HFpEF at peak exercise (Table 3). Absence of between group differences for other metrics at rest persisted to peak exercise. For within group differences from rest to peak exercise, HFrEF and HFpEF demonstrated similar directional changes for variables in Table 3 except for PaO_2, which increased within HFrEF but not within HFpEF.

In sub-analyses including only HFrEF (N=22) and HFpEF (N=17) on β_1-blockers, between-within differences for $\dot{V}_E/\dot{V}CO_2$ slope (F=13.7, P<0.01), V_D/V_T (F=20.7, P<0.01), and $PaCO_2$ (F=5.12, P<0.01) mirrored outcomes illustrated in Figure 1(A–C). Within HFpEF, there were no differences in $\dot{V}_E/\dot{V}CO_2$ slope (P=0.96), peak exercise V_D/V_T (P=0.69), and peak exercise $PaCO_2$ (P=0.90) between patients on versus not on β_1-blockers.

Predictors of $\dot{V}_E/\dot{V}CO_2$ slope

Resting LVEF was unrelated to $\dot{V}_E/\dot{V}CO_2$ slope when stratified by HF group (Figure 1D), whereas combining all HF resulted in a modest relationship ($y=-0.21x+48$, $R^2=0.16$,

P=0.01). In comparison, peak exercise V_D/V_T and $PaCO_2$ strongly explained the variance in $\dot{V}_E/\dot{V}CO_2$ slope across all HF (Figure 1E and 1F).

Consistent with plots of HFrEF versus HFpEF in Figures 1E and 1F, unique contributions from each group to pooled regressions are illustrated in detail in Figure 2. While decreasing $PaCO_2$ strongly explained the variance associated with increasing $\dot{V}_E/\dot{V}CO_2$ slope in HFrEF (Figure 2B), V_D/V_T was more strongly related to elevated $\dot{V}_E/\dot{V}CO_2$ slope in HFpEF (Figure 2C). Although there was significant linearity between increasing V_D/V_T and $\dot{V}_E/\dot{V}CO_2$ slope in HFrEF (Figure 2A) as well as $PaCO_2$ and $\dot{V}_E/\dot{V}CO_2$ slope (Figure 2D, inverse relationship) in HFpEF, variance explained in Figures 2A and 2D was approximately half of Figures 2B and 2C in HFrEF and HFpEF, respectively. In the absence of V_D/V_T (Y-intercept not different from 0.0, *P*=0.14; Figure 2A), and not until V_D/V_T >0.2, was $\dot{V}_E/\dot{V}CO_2$ slope elevated except for the influence of $PaCO_2$ in HFrEF (Figure 2B). In contrast, V_D/V_T accompanied by lesser effects from $PaCO_2$ contributed to increased $\dot{V}_E/\dot{V}CO_2$ slope at $V_D/V_T \geq 1.0$ in HFpEF (Figure 2C; and Figure 2D isopleths).

Finally, while increasing $\dot{V}_D$ and PAO_2 accompanied by decreasing $PACO_2$ demonstrated significant linearity with increasing $\dot{V}_E/\dot{V}CO_2$ slope in HFrEF and HFpEF, in an inverse manner, HCO_3^- and BE explained the variance in $\dot{V}_E/\dot{V}CO_2$ slope in HFrEF, whereas this did not occur in HFpEF (Table 4).

Discussion

These data suggest increased $\dot{V}_E/\dot{V}CO_2$ slope in both HFrEF and HFpEF patients is fundamentally linked to elevated V_D/V_T accompanied by altered regulation of $PaCO_2$ during CPET. Both HFrEF and HFpEF demonstrated $\dot{V}_E/\dot{V}CO_2$ slope at levels consistent with worsened prognosis (1–4). However, moderate-to-strong relationships between increasing V_D/V_T and decreasing $PaCO_2$ with rising $\dot{V}_E/\dot{V}CO_2$ slope differed in HFrEF compared to HFpEF. Decreasing $PaCO_2$ at peak exercise in HFrEF explained >2× the variance in $\dot{V}_E/\dot{V}CO_2$ slope compared to the same relationship tested in HFpEF. By contrast, despite demonstrating lower peak exercise V_D/V_T compared to HFrEF, variance explained between increasing V_D/V_T and $\dot{V}_E/\dot{V}CO_2$ slope in HFpEF was >1.5× that of HFrEF. These data are consistent with the hypothesis that increased $\dot{V}_E/\dot{V}CO_2$ slope is not exclusively a function of central hemodynamic limitations in patients with HFrEF or HFpEF (4, 5, 18–20).

While abnormal V_D/V_T and $PaCO_2$ contribute to increased $\dot{V}_E/\dot{V}CO_2$ (slope/ratio) in HFrEF (4, 7, 9, 10), these relationships have not been tested in HFpEF. These data in HFrEF are consistent with work from Guazzi et al. (4) and Woods et al. (7) who during peak and submaximal CPET, demonstrated low $PaCO_2$ and high V_D/V_T paralleled increased $\dot{V}_E/\dot{V}CO_2$ in HFrEF. By comparison, these observations are in contrast to interpretations of others (9, 10) suggesting $PaCO_2$ coupled to ventilatory control mechanisms are not altered in HFrEF; instead, suggesting increased $\dot{V}_E/\dot{V}CO_2$ slope is related to high V_D/V_T provoked by impaired pulmonary perfusion and, hence, $\dot{V}_A/\dot{Q}$ >1.0. Although this study did not include specific tests of ventilatory control related to chemoreflexes and/or group III/IV muscle afferents, these data align with several related studies in HF suggesting neurophysiologic

control pathways abnormally activated during increased energy demand may play an appreciable role in excessive ventilatory responses to exercise in HF (4, 7, 18–21).

Energy demand in-excess of oxidative capabilities leads to a marked rise in CO_2 production followed by an acidotic blood milieu if accumulated CO_2 blood content is not adequately compensated (6, 8). In healthy adults, metabolic-driven production of CO_2 leads to intrinsic activation of pathways relating to mechanisms of HCO_3^- formation accompanied by increased ventilation. Timely coordination of these events during exercise functions well as a buffering mechanism (Hb binds H^+) to help maintain blood acid-base balance while facilitating decreased blood CO_2 content as Na^+ binds HCO_3^- (and to a lesser extent Hb binds CO_2) to be transported to the pulmonary system for expiration. However, it remains unclear how these interconnected compensatory mechanisms of breathing and acid-base buffering equilibrate in conditions where both the rate and absolute level of CO_2 accumulation in blood may become accelerated, such as might occur in HF.

Patients with HF demonstrate greater reliance on nonoxidative energy demand leading to increased CO_2 production (20). Both HFrEF and HFpEF may demonstrate skeletal muscle fiber shifts leading to an increased proportion of type II (glycolytic) relative type I fibers, decreased mitochondrial density and enzymatic activity, and exacerbated central chemoreceptor and/or group III/IV afferent activation via elevated circulating H^+ (18–21). Thus, these and other pathologic events proposed in HF are compatible with augmented blood CO_2 content and low pHa, which could be expected to provoke augmented ventilatory compensation.

The rate of increase in $\dot{V}_E$ relative to metabolic demand was exaggerated across our HF patients. Likewise, a formidable drop in HCO_3^- from rest to peak exercise accompanied by negative BE is consistent with the presence of metabolic acidosis and base deficit (6, 8, 22, 23). The concurrent decrease in $PaCO_2$ linked to patterned responses in HCO_3^-, BE, $\dot{V}_E$, and pHa is consistent with the notion that ventilatory control pathways may function at an abnormally high gain coupled with a low $PaCO_2$ (apneic) set-point in HF (4). In this context, our group and others have demonstrated that metabolically activated muscle afferents during exercise contribute to increased ventilation and $\dot{V}_E/\dot{V}CO_2$ slope in HFrEF (18, 19, 21). While this study did not include tests of muscle afferent activation linked to ventilatory function, assuming skeletal muscle pathology occurs secondary to HF (20), this musculoskeletal neural pathway connecting systemic blood biochemical changes to brainstem centers of ventilatory control is a candidate mechanism contributing to increased $\dot{V}_E/\dot{V}CO_2$ slope in HF.

Although $PaCO_2$ and V_D/V_T are interrelated, the shift in the relationship between increased $\dot{V}_E/\dot{V}CO_2$ slope from $PaCO_2$ in HFrEF to V_D/V_T in HFpEF suggests there may have been an influence of sub-clinical pathology of mechanical and/or structural pulmonary features on increased $\dot{V}_E/\dot{V}CO_2$ slope in HFpEF (4, 9, 15, 24). However, if sub-clinical pulmonary disease occurring independently or secondary to HF were to have been present in HFpEF, we hypothesize that while inhomogeneous distribution of $\dot{V}_A/\dot{Q}$ >1.0 lung units may have contributed to increased V_D/V_T and $\dot{V}_E/\dot{V}CO_2$ slope (9, 10), the stronger influence of $\dot{V}_A/\dot{Q}$ on high V_D/V_T would have derived from effects of $\dot{V}_A/\dot{Q}$ <1.0 (suggested by $PECO_2$/

$P_{ET}CO_2$ ≤0.70 (15)). Even with the potential for moderately reduced (~20% drop from normal) lung diffusing capacity in HFpEF (24), because of distinct properties of CO_2 (e.g., high blood solubility and diffusion rate) it could be suggested that *any* perfusion ($\dot{V}_A/\dot{Q}$ >0.0) of normally ventilated alveoli will result in little interference in CO_2 transfer (6, 8). In contrast, it is likely that with inhomogeneous distribution of $\dot{V}_A/\dot{Q}$ <1.0, $\dot{V}_A$, and DLO_2 throughout lungs that effects of venous admixture and moderately reduced gas transfer could be expected to nominally influence $PaCO_2$ while effectively diluting arterial O_2 content and increase $PA\text{-}aO_2$. Inasmuch as HFpEF demonstrated alignment between $PaCO_2$ and $PACO_2$ suggesting no impairment in CO_2 diffusing capacity, $PA\text{-}aO_2$ simultaneously extended beyond normal limits (6, 8). These combined observations are consistent with the suggestion that $\dot{V}_A/\dot{Q}$ <1.0 lung areas demonstrate stronger effects on PaO_2 compared to effects of $\dot{V}_A/\dot{Q}$ >1.0 lung sectors on impaired CO_2 exchange and, hence, $PaCO_2$ (6, 8). Thus, although peak exercise $PaCO_2$ inversely related to $\dot{V}_E/\dot{V}CO_2$ slope in HFpEF, it does not appear that effects of abnormal pulmonary CO_2 transfer and whole lung $\dot{V}_A/\dot{Q}$ >1.0 played an appreciable role in this relationship.

Limitations

Information regarding the long-term prognostic translation of the present observations is not yet available in this limited sample size of HF patients, and causality cannot be deduced from these data. Increased $\dot{V}_E/\dot{V}CO_2$ slope in HFpEF of this study represents the higher limit in this population. A possible explanation for this observation is a secondary effect of aging as these data are consistent with reports of Haykowski et al. (5) and Borlaug et al. (12) in HFpEF of similar age, whereas younger HFpEF in Shafiq et al. (2) and Guazzi et al. (1) demonstrated lesser $\dot{V}_E/\dot{V}CO_2$ slope. Additional effects of obesity might also be considered impactful to increased $\dot{V}_E/\dot{V}CO_2$ slope secondary to attenuated pulmonary perfusion as others have demonstrated direct correlation between BMI and degree of diastolic dysfunction independent of comorbidities commonly recognized in HFpEF (25). While this study did not include age and body sized matched controls with respect to each HF group, elucidating the independent influences of aging and obesity on ventilatory inefficiency is important in this line of study as both factors contribute to the HFpEF phenotype.

Discussions regarding the influence of pulmonary perfusion on $\dot{V}_E/\dot{V}CO_2$ slope and V_D/V_T are hypothesis generating interpretations without direct measurements of central hemodynamics. Despite this limitation, the study design based upon ‘ideal’ alveolar equations accounts for cardiopulmonary hemodynamic interactions in addition to influences of peripheral perfusion physiology on the derivation of $\dot{V}_E/\dot{V}CO_2$ slope (4, 6–9). Although $PaCO_2$ is taken as a cross-sectional measurement, whereas $\dot{V}_E/\dot{V}CO_2$ slope is quantified as a continuous variable, we suggest breath-to-breath variability in $PaCO_2$ (i.e., negligible compared to inter-breath variability in $P_{ET}CO_2$) would not have an appreciable effect on relationships demonstrated in this study.

We acknowledge that β-blocker selectivity may potentially impact the interpretation of $\dot{V}_E/\dot{V}CO_2$ slope in HFrEF (26). This study was not powered to test the effect of β-blocker selectivity on our outcomes, and therefore additional studies are needed to clarify the potential role of β-blocker selectivity on exercise ventilation in HF. The immediate

translation of these data to a specific therapeutic strategy to improve ventilatory efficiency in HF is also not yet available. However, based on recent observations in HFpEF suggesting exercise training attenuates pathologic processes of skeletal muscle remodeling (leading to improved oxidative metabolism (27)) and exercise accompanied by inorganic nitrite supplementation improves central—peripheral hemodynamics (e.g., $\dot{V}_A/\dot{Q}$ ~1.0) (12, 28), we hypothesize that questions tested in this study applied to those paradigms can be used to advance the understanding of how to interpret $\dot{V}_E/\dot{V}CO_2$ slope while also lending an ability to properly manage ventilatory function in HF. Lastly, our suggestion of a possible role of impaired skeletal muscle afferents on abnormal ventilatory control that contributes to increased $\dot{V}_E/\dot{V}CO_2$ slope in HFpEF has not been formally tested in the setting of the present aims. However, because of skeletal muscle pathophysiology (e.g., shift from type I to II fibers (20)), HFpEF may be predisposed to abnormal skeletal muscle afferent function similar to that recognized in HFrEF (18, 19, 21).

Conclusions

These data suggest patients with HF demonstrate abnormally increased $\dot{V}_E/\dot{V}CO_2$ slope, which can be explained by both V_D/V_T and $PaCO_2$ during CPET. However, variance in $\dot{V}_E/\dot{V}CO_2$ slope is more strongly explained by V_D/V_T than $PaCO_2$ in HFpEF as compared to HFrEF patients, in whom variance in $\dot{V}_E/\dot{V}CO_2$ slope can be primarily accounted for by decreased $PaCO_2$. These hypothesis-generating data emphasize the need to refine the interpretation and clinical utility of $\dot{V}_E/\dot{V}CO_2$ slope in HF. Advanced studies focusing on the integrated pathophysiology of abnormal $\dot{V}_E/\dot{V}CO_2$ slope, V_D/V_T, and $PaCO_2$ are warranted in HF, particularly those examining the unique relevance of peripheral musculoskeletal pathologies in contributing to the variable HF phenotype which has come to the forefront in discussions of HFpEF (1–3, 5, 11, 12, 20).

Acknowledgments

The authors would like to acknowledge and thank all participants who volunteered for this study.

Sources of Funding

Funding for this work was supported by National Institutes of Health [HL126638 to TPO; HL071478 to BDJ; and HL128526 and U10 HL110262 to BAB]; and American Heart Association [16POST30260021 to EHV].

References

1. Guazzi M, Myers J, Arena R. Cardiopulmonary exercise testing in the clinical and prognostic assessment of diastolic heart failure. J Am Coll Cardiol. 2005 Nov 15; 46(10):1883–1890. [PubMed: 16286176]
2. Shafiq A, Brawner CA, Aldred HA, Lewis B, Williams CT, Tita C, Schairer JR, Ehrman JK, Velez M, Selektor Y, Lanfear DE, Keteyian SJ. Prognostic value of cardiopulmonary exercise testing in heart failure with preserved ejection fraction. The Henry Ford HospITal CardioPulmonary EXercise Testing (FIT-CPX) project. Am Heart J. 2016 Apr.174:167–172. [PubMed: 26995385]
3. Nedeljkovic I, Banovic M, Stepanovic J, Giga V, Djordjevic-Dikic A, Trifunovic D, Nedeljkovic M, Petrovic M, Dobric M, Dikic N, Zlatar M, Beleslin B. The combined exercise stress echocardiography and cardiopulmonary exercise test for identification of masked heart failure with preserved ejection fraction in patients with hypertension. Eur J Prev Cardiol. 2016 Jan; 23(1):71–77. [PubMed: 26358991]

4. Guazzi M, Reina G, Tumminello G, Guazzi MD. Exercise ventilation inefficiency and cardiovascular mortality in heart failure: the critical independent prognostic value of the arterial CO2 partial pressure. Eur Heart J. 2005 Mar; 26(5):472–480. [Research Support, Non-U.S. Gov't]. [PubMed: 15618042]
5. Haykowsky MJ, Brubaker PH, John JM, Stewart KP, Morgan TM, Kitzman DW. Determinants of exercise intolerance in elderly heart failure patients with preserved ejection fraction. J Am Coll Cardiol. 2011 Jul 12; 58(3):265–274. [PubMed: 21737017]
6. Riley RL, Cournand A. Analysis of factors affecting partial pressures of oxygen and carbon dioxide in gas and blood of lungs; theory. J Appl Physiol. 1951 Aug; 4(2):77–101. [PubMed: 14888620]
7. Woods PR, Olson TP, Frantz RP, Johnson BD. Causes of breathing inefficiency during exercise in heart failure. J Card Fail. 2010 Oct; 16(10):835–842. [Research Support, N.I.H., Extramural]. [PubMed: 20932466]
8. Wasserman K, Van Kessel AL, Burton GG. Interaction of physiological mechanisms during exercise. J Appl Physiol. 1967 Jan; 22(1):71–85. [PubMed: 6017656]
9. Sullivan MJ, Higginbotham MB, Cobb FR. Increased exercise ventilation in patients with chronic heart failure: intact ventilatory control despite hemodynamic and pulmonary abnormalities. Circulation. 1988 Mar; 77(3):552–559. [PubMed: 3342486]
10. Wensel R, Francis DP, Georgiadou P, Scott A, Genth-Zotz S, Anker SD, Coats AJ, Piepoli MF. Exercise hyperventilation in chronic heart failure is not caused by systemic lactic acidosis. European journal of heart failure. 2005; 7(7):1105–1111. [PubMed: 16326362]
11. De Keulenaer GW, Brutsaert DL. Systolic and Diastolic Heart Failure Are Overlapping Phenotypes Within the Heart Failure SpectrumResponse to De Keulenaer and Brutsaert. Circulation. 2011; 123(18):1996–2005. [PubMed: 21555722]
12. Borlaug BA, Melenovsky V, Koepp KE. Inhaled Sodium Nitrite Improves Rest and Exercise Hemodynamics in Heart Failure With Preserved Ejection Fraction. Circ Res. 2016 Sep 16; 119(7): 880–886. [PubMed: 27458234]
13. McMurray JJ, Adamopoulos S, Anker SD, Auricchio A, Böhm M, Dickstein K, Falk V, Filippatos G, Fonseca C, Gomez-Sanchez MA. ESC Guidelines for the diagnosis and treatment of acute and chronic heart failure 2012. European journal of heart failure. 2012; 14(8):803–869. [PubMed: 22828712]
14. Hansen JE, Sue DY, Wasserman K. Predicted values for clinical exercise testing. Am Rev Respir Dis. 1984 Feb; 129(2 Pt 2):S49–55. [PubMed: 6421218]
15. Hansen JE, Ulubay G, Chow BF, Sun XG, Wasserman K. Mixed-expired and end-tidal CO2 distinguish between ventilation and perfusion defects during exercise testing in patients with lung and heart diseases. Chest. 2007 Sep; 132(3):977–983. [PubMed: 17573506]
16. Arena R, Myers J, Aslam SS, Varughese EB, Peberdy MA. Technical considerations related to the minute ventilation/carbon dioxide output slope in patients with heart failure. Chest. 2003 Aug; 124(2):720–727. [PubMed: 12907564]
17. Cohen J. A power primer. Psychol Bull. 1992 Jul; 112(1):155–159. [PubMed: 19565683]
18. Ponikowski PP, Chua TP, Francis DP, Capucci A, Coats AJ, Piepoli MF. Muscle ergoreceptor overactivity reflects deterioration in clinical status and cardiorespiratory reflex control in chronic heart failure. Circulation. 2001 Nov 6; 104(19):2324–2330. [Clinical Trial Controlled Clinical Trial Research Support, Non-U.S. Gov't]. [PubMed: 11696473]
19. Scott AC, Francis DP, Davies LC, Ponikowski P, Coats AJ, Piepoli MF. Contribution of skeletal muscle 'ergoreceptors' in the human leg to respiratory control in chronic heart failure. J Physiol. 2000; 529(3):863–870. [PubMed: 11118512]
20. Kitzman DW, Nicklas B, Kraus WE, Lyles MF, Eggebeen J, Morgan TM, Haykowsky M. Skeletal muscle abnormalities and exercise intolerance in older patients with heart failure and preserved ejection fraction. Am J Physiol Heart Circ Physiol. 2014 May; 306(9):H1364–1370. [PubMed: 24658015]
21. Olson TP, Joyner MJ, Eisenach JH, Curry TB, Johnson BD. Influence of locomotor muscle afferent inhibition on the ventilatory response to exercise in heart failure. Exp Physiol. 2014 Feb; 99(2): 414–426. [Randomized Controlled Trial Research Support, N.I.H., Extramural Research Support, Non-U.S. Gov't]. [PubMed: 24163425]

22. Andersen OS. Blood acid-base alignment nomogram. Scales for pH, pCO2 base excess of whole blood of different hemoglobin concentrations, plasma bicarbonate, and plasma total-CO2. Scand J Clin Lab Invest. 1963; 15:211–217. [PubMed: 14012796]
23. Siggaard-Andersen O. The van Slyke equation. Scand J Clin Lab Invest Suppl. 1977; 146(sup146): 15–20. [PubMed: 13478]
24. Olson TP, Johnson BD, Borlaug BA. Impaired Pulmonary Diffusion in Heart Failure With Preserved Ejection Fraction. JACC Heart Fail. 2016 Jun; 4(6):490–498. [PubMed: 27256752]
25. Russo C, Jin Z, Homma S, Rundek T, Elkind MS, Sacco RL, Di Tullio MR. Effect of obesity and overweight on left ventricular diastolic function: a community-based study in an elderly cohort. Journal of the American College of Cardiology. 2011; 57(12):1368–1374. [PubMed: 21414533]
26. Witte KK, Thackray S, Nikitin NP, Cleland JG, Clark AL. The effects of long-term β-blockade on the ventilatory responses to exercise in chronic heart failure. European journal of heart failure. 2005; 7(4):612–617. [PubMed: 15921802]
27. Pandey A, Parashar A, Kumbhani D, Agarwal S, Garg J, Kitzman D, Levine B, Drazner M, Berry JD. Exercise training in patients with heart failure and preserved ejection fraction: a meta-analysis of randomized control trials. Circulation: Heart Failure. 2014 CIRCHEARTFAILURE. 114.001615.
28. Borlaug BA, Koepp KE, Melenovsky V. Sodium Nitrite Improves Exercise Hemodynamics and Ventricular Performance in Heart Failure With Preserved Ejection Fraction. J Am Coll Cardiol. 2015 Oct 13; 66(15):1672–1682. [PubMed: 26449137]
29. Van Slyke DD, Sendroy J, Hastings AB, Neill JM. STUDIES OF GAS AND ELECTROLYTE EQUILIBRIA IN BLOOD X. THE SOLUBILITY OF CARBON DIOXIDE AT 38° IN WATER, SALT SOLUTION, SERUM, AND BLOOD CELLS. Journal of Biological Chemistry. 1928; 78(3):765–799.
30. Severinghaus JW. Blood gas calculator. J Appl Physiol. 1966 May; 21(3):1108–1116. [PubMed: 5912737]

Appendix: Calculation methods for derived blood biochemistry and 'ideal' alveolar (gas/air) equation parameters

In using arterialized blood draws as described in the above text (methods), the Henderson-Hasselbalch equation was used to derive bicarbonate (HCO_3^-) in blood as,

$$\mathrm{HCO_3^-} = s \times \mathrm{PaCO_2} \times 10^{\mathrm{pHa}-\mathrm{pK}'};$$

where at standard body temperature of 37°C and pHa at 7.4, s equals 0.0307 mmol/L/mm Hg, which is the plasma solubility coefficient of CO_2, whereas pK' equals 6.0907, which is the acid-dissociation constant of carbonic acid (29, 30). Both s and pK' were corrected for temperature (T) and pHa as follows (29, 30):

$$s = 0.0307 + 0.00057 \times (37 - \mathrm{T}) + 0.0002 \times (37 - \mathrm{T})^2, \text{and}$$
$$\mathrm{p}K' = 6.086 + 0.042 \times (7.4 - \mathrm{pHa}) + (38 - \mathrm{T}) \times [0.00472 + 0.00139 \times (7.4 - \mathrm{pHa})]$$

Base excess of arterialized blood (BE) was calculated using the Van Slyke equation derived by Siggaard-Andersen from BE and buffer base curves at body temperature and corrected for SaO_2 (22, 23),

$$\mathrm{BE}=\left[\mathrm{Z}\times\left(\left(\mathrm{HCO}_3^-{-}24.4\right)+\beta\times\left(\mathrm{pHa}-7.4\right)\right)\right]+\left[0.3\times\mathrm{Hb}\times\frac{100-\mathrm{SaO}_2}{100}\right];$$

where Z describes the distribution of HCO_3^- between red blood cells and plasma depending on hemoglobin (Hb) concentration equal to, 1–0.0143×Hb; 24.4 is the plasma HCO_3^- concentration at a reference pHa of 7.4; β is the slope constant of the HCO_3^- vs. pHa plot equal to, 7.7+1.43×Hb; and the final bracketed term is to correct for differences in SaO_2 from ideal oxygenation at 1.0.

Derived alveolar gas and air equation parameters

By using arterial blood gas measurements and acquired basic ventilation and gas exchange responses, 'ideal' alveolar gas and air equations and associated parameters could be used to calculate the following in addition to V_D/V_T (as explained above in methods) (4, 6, 7, 9, 10): alveolar ventilation and volume,

$$\dot{\mathrm{V}}_\mathrm{A}=\dot{\mathrm{V}}_\mathrm{E}\times\left(1-\frac{\mathrm{V}_\mathrm{D}}{\mathrm{V}_\mathrm{T}}\right)\ \text{and}\ \mathrm{V}_\mathrm{A}=\frac{\dot{\mathrm{V}}_\mathrm{A}}{f_\mathrm{B}},\text{respectively};$$

alveolar CO_2 tension,

$$\mathrm{PACO}_2=\frac{863\times\dot{\mathrm{V}}\ \mathrm{CO}_2}{\dot{\mathrm{V}}_\mathrm{A}};$$

alveolar O_2 tension,

$$\mathrm{PAO}_2=\mathrm{P}_\mathrm{I}\mathrm{O}_2+\frac{\mathrm{PACO}_2\times0.21\times(1-\mathrm{RER})}{100\times\mathrm{RER}}-\frac{\mathrm{PACO}_2}{\mathrm{RER}};$$

ventilation of V_D ($\dot{V}_D$),

$$\dot{\mathrm{V}}_\mathrm{D}=\dot{\mathrm{V}}_\mathrm{E}-\dot{\mathrm{V}}_\mathrm{A};$$

and alveolar-to-arterial O_2 difference (PA-aO_2) was calculated as the difference between PAO_2 and PaO_2. To account for potential effects of differences in absolute $\dot{V}O_2$ on the interpretability of PA-aO_2, we also provide PA-aO_2 standardized to $\dot{V}O_2$ (PA-$aO_2/\dot{V}O_2$).

Because of complexities involved in properly deriving end-pulmonary capillary O_2 tension, we provide an indirect simplified estimate of whole lung diffusion capacity for O_2 via Fick's law of diffusion,

$$DLO_2 = \frac{\dot{V}\ O_2}{PAO_2 - PaO_2}.$$

For above parameters related to 'ideal' alveolar gas and air equations: $\dot{V}_E$ is minute ventilation, V_D is physiologic dead space, V_T is tidal volume, f_B is respiratory rate, $\dot{V}CO_2$ is carbon dioxide output, 863 is the correction factor needed when computing partial pressure from fractional concentration involving both volumes/gas (STPD) and volumes/flows (BTPS, body temperature and pressure, saturated) standards of measurement, P_IO_2 is the inspired tension of O_2, 0.21 is inspired O_2 fraction (room air), RER is the respiratory exchange ratio at the lung, $\dot{V}O_2$ is pulmonary O_2 uptake, and PaO_2 is arterial O_2 tension.

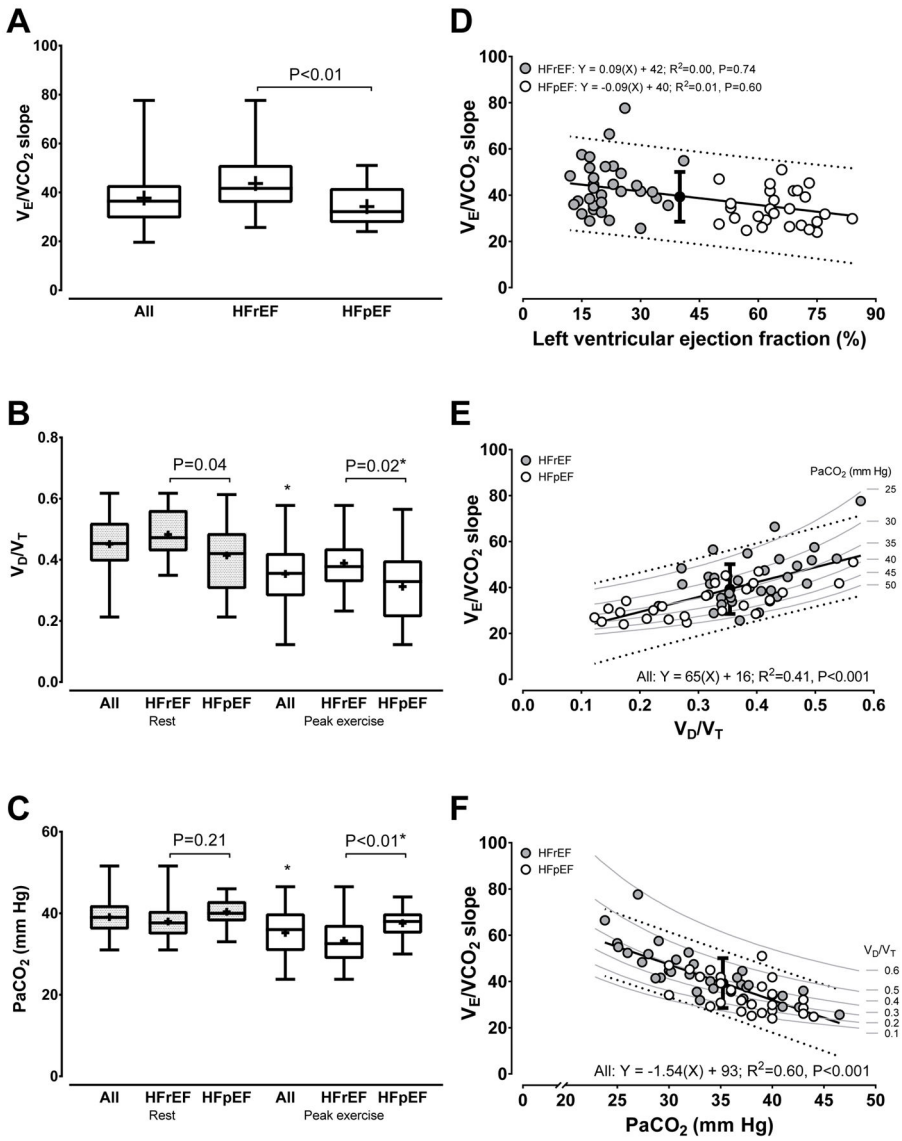

Figure 1.

Measurements or univariate linear regressions involving the ventilatory equivalent for carbon dioxide ($\dot{V}_E/\dot{V}CO_2$) slope, physiologic dead space to tidal volume ratio (V_D/V_T), or arterial carbon dioxide tension ($PaCO_2$). Data presented in panels A to C are interquartile range with mean represented as (+). Variables presented on the abscissa in panels D to F are at rest, peak exercise, and peak exercise, respectively. For panels D to F representative of all participants: filled circle is mean ± SD of $\dot{V}_E/\dot{V}CO_2$ slope at the mean of the variable set on the abscissa, solid line is goodness of fit line of the model fit equation, dotted lines are 95% prediction bands of the model fit equation, and grey bands are isopleths representing linked changes in observed $\dot{V}_E/\dot{V}CO_2$ slope and $PaCO_2$ or V_D/V_T when either $PaCO_2$ or V_D/V_T are theoretically constrained values. Interpretation of R^2: modest=0.02; moderate=0.15; or strong≥0.25. The Y-intercept in panels D to F differed from 0.0 (P<0.01). Differences in R^2: panel D vs. E or F, P<0.001; panel E vs. F, P=0.16. Heart failure with reduced (HFrEF, N=32) or preserved (HFpEF, N=27) ejection fraction. *Following post-hoc Tukey-Kramer

testing, different within group for both HFrEF and HFpEF or all HF, rest to peak exercise, $P<0.05$.

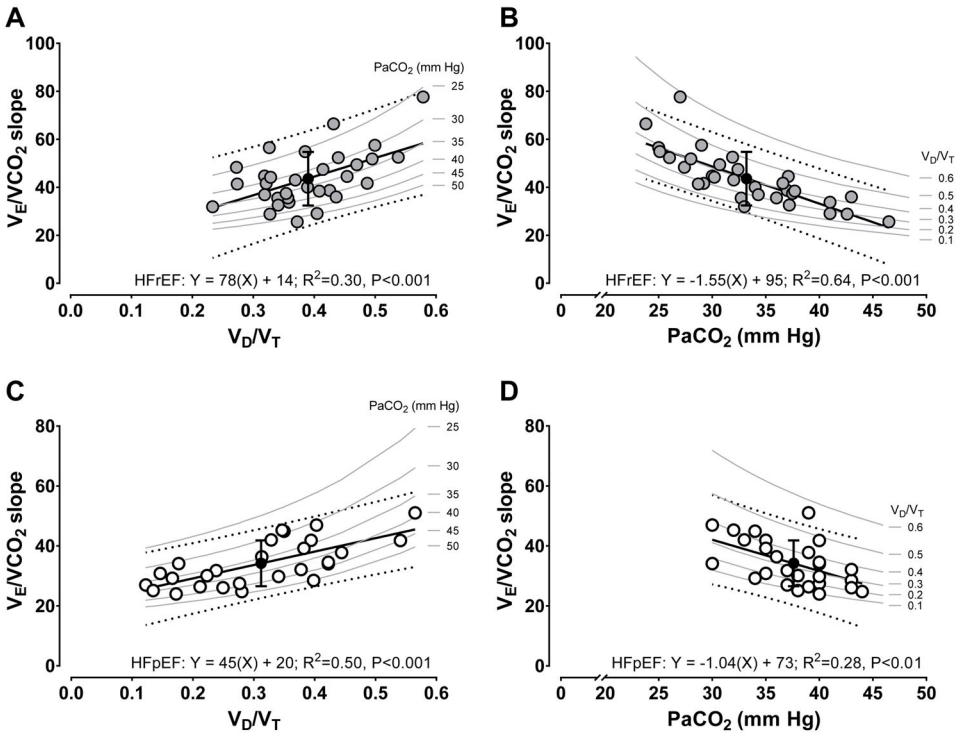

Figure 2.

Univariate linear regressions involving the ventilatory equivalent for carbon dioxide ($\dot{V}_E/\dot{V}CO_2$) slope (dependent, ordinate), peak exercise physiologic dead space to tidal volume ratio (V_D/V_T) (independent, abscissa), or peak exercise arterial CO_2 tension ($PaCO_2$) (independent, abscissa). For all panels: filled circle is mean ± SD of $\dot{V}_E/\dot{V}CO_2$ slope at the mean of the variable set on the abscissa, solid line is goodness of fit line of the model fit equation, dotted lines are 95% prediction bands of the model fit equation, and grey bands are isopleths representing linked changes in observed $\dot{V}_E/\dot{V}CO_2$ slope and $PaCO_2$ or V_D/V_T when either $PaCO_2$ or V_D/V_T are theoretically constrained values. Interpretation of R^2: modest=0.02; moderate=0.15; or strong≥0.25. The Y-intercept in panel A did not differ from 0.0 (*P*=0.14), whereas the Y-intercept in panels B to D differed from 0.0 (*P*<0.01). Differences in R^2: panel A vs. B, *P*=0.06; panel A vs. C, *P*=0.33; panel B vs. D, *P*=0.06; panel C vs. D, *P*=0.30. Heart failure with reduced (HFrEF, N=32) or preserved (HFpEF, N=27) ejection fraction.

Table 1

Participant characteristics

	All	HFrEF	HFpEF	*P*-value
Variable	N = 59	N = 32	N = 27	
Age (years)	62 ± 13	55 ± 10	71 ± 11	<0.001
Sex (male/female)	46/13	30/2	16/11	<0.001
LV ejection fraction (%)	40 ± 21	22 ± 7	61 ± 9	<0.001
NYHA class, n (%)				
II	20 (34)	13 (41)	7 (26)	0.07
III	39 (66)	19 (59)	20 (74)	0.19
Height (cm)	172 ± 9	174 ± 8	170 ± 10	0.14
Weight (kg)	92 ± 20	86 ± 15	96 ± 23	0.05
Body mass index (kg/m^2)	30 ± 6	28 ± 4	33 ± 6	<0.01
Body surface area (m^2)	2.07 ± 0.26	2.03 ± 0.21	2.12 ± 0.31	0.19
Peak $\dot{V}O_2$ (% of pred.)	39 ± 14	31 ± 7	50 ± 14	<0.001
Peak $\dot{V}O_2$ (mL/kg/min)	8.6 ± 2.3	8.3 ± 2.2	8.8 ± 2.4	0.46
Weber-Janicki class [peak $\dot{V}O_2$], n (%)				
C, 10–16 mL/kg/min	14 (24)	7 (22)	7 (26)	0.88
D, <10 mL/kg/min	45 (76)	25 (78)	20 (74)	0.75
Hemoglobin (g/dL)	13.3 ± 1.7	13.9 ± 1.6	12.5 ± 1.4	0.01
Creatinine (mg/dL)	1.33 ± 0.42	1.39 ± 0.40	1.26 ± 0.43	0.23
eGFR (mL/min per 1.73 m^2)	56 ± 15	56 ± 15	55 ± 16	0.80
Drug Therapy, n (%)				
ACE inhibitor	37 (63)	25 (78)	12 (44)	<0.001
ARBs	9 (15)	2 (6)	7 (26)	<0.001
Antiarrhythmic	15 (25)	10 (31)	5 (19)	0.09
β-blocker (β_1 or non-select.)	45 (76)	28 (88)	17 (63)	0.04
Ca^{2+} channel blocker	7 (12)	1 (3)	6 (22)	<0.001
Digoxin	25 (42)	23 (72)	2 (7)	<0.001
Nitrate (oral, SL, or topical)	19 (32)	9 (28)	10 (33)	0.52
Aspirin	43 (73)	22 (69)	21 (78)	0.46
Diuretics	40 (68)	29 (91)	11 (41)	<0.001
Echocardiography				
LA volume (mL)	104 ± 43	115 ± 42	84 ± 40	0.03
LA volume index (mL/m^2)	51 ± 20	56 ± 20	43 ± 20	0.04
Mitral E-wave VEL (cm/s)	89.3 ± 30.1	89.3 ± 40.1	89.3 ± 22.2	0.58
Mitral A-wave VEL (cm/s)	68.9 ± 29.7	59.0 ± 32.8	77.5 ± 24.2	0.01
Mitral E/A ratio	1.4 ± 0.8	1.7 ± 0.9	1.2 ± 0.6	0.11
Mitral septal tissue Doppler VEL (e′) (cm/s)	5.3 ± 1.8	4.5 ± 1.7	6.1 ± 1.7	<0.001
Mitral E/e′ ratio	19.1 ± 9.8	22.1 ± 10.9	16.2 ± 7.7	0.02
IV septum thickness (mm)	9.9 ± 1.6	9.5 ± 1.6	10.2 ± 1.6	0.06

	All	HFrEF	HFpEF	*P*-value
Posterior wall thickness (mm)	9.8 ± 1.7	9.7 ± 1.5	9.9 ± 1.9	0.96

Data are mean ± SD, n, or percentage (%).

Table 2

Basic ventilatory and gas exchange responses at rest and peak exercise

	All	HFrEF	HFpEF	*P*-value
Rest	N = 59	N = 32	N = 27	
$\dot{V}O_2$ (L/min)	0.24 ± 0.06	0.23 ± 0.05	0.25 ± 0.07	0.97
$\dot{V}CO_2$ (L/min)	0.21 ± 0.06	0.20 ± 0.05	0.21 ± 0.07	0.99
RER	0.87 ± 0.10	0.88 ± 0.10	0.85 ± 0.09	0.63
$\dot{V}_E$ (L/min)	8.6 ± 2.7	9.0 ± 2.2	8.1 ± 3.3	0.95
f_B (breaths/min)	17 ± 4	17 ± 4	16 ± 5	0.91
V_T (L)	0.54 ± 0.18	0.54 ± 0.16	0.53 ± 0.20	0.99
$\dot{V}_E/\dot{V}CO_2$	42 ± 8	45 ± 7	38 ± 6	<0.001
$P_{ET}O_2$ (mm Hg)	103 ± 6	103 ± 6	102 ± 5	0.98
$P_{ET}CO_2$ (mm Hg)	35 ± 6	33 ± 5	39 ± 5	<0.001
$PECO_2$ (mm Hg)	21 ± 4	20 ± 3	23 ± 4	<0.01
$PECO_2/P_{ET}CO_2$	0.60 ± 0.06	0.61 ± 0.06	0.60 ± 0.06	0.98
Peak exercise				
Workload, W	38 ± 11	39 ± 11	36 ± 12	0.39
$\dot{V}O_2$ (L/min)	0.76 ± 0.22 *	0.70 ± 0.18 *	0.82 ± 0.25 *	0.04
$\dot{V}CO_2$ (L/min)	0.82 ± 0.23 *	0.77 ± 0.19 *	0.89 ± 0.25 *	0.04
RER	1.10 ± 0.08 *	1.10 ± 0.09 *	1.10 ± 0.06 *	0.92
$\dot{V}_E$ (L/min)	32 ± 9 *	33 ± 9 *	35 ± 9 *	0.43
f_B (breaths/min)	31 ± 8 *	30 ± 7 *	31 ± 10 *	0.97
V_T (L)	1.08 ± 0.33 *	1.13 ± 0.35 *	1.03 ± 0.31 *	0.43
$\dot{V}_E/\dot{V}CO_2$	40 ± 10	44 ± 10	35 ± 7 *	<0.001
$P_{ET}O_2$ (mm Hg)	112 ± 7 *	113 ± 7 *	111 ± 6 *	0.62
$P_{ET}CO_2$ (mm Hg)	34 ± 8	30 ± 6 *	39 ± 7	<0.001
$PECO_2$ (mm Hg)	23 ± 5	20 ± 4	25 ± 5 *	<0.01
$PECO_2/P_{ET}CO_2$	0.68 ± 0.05 *	0.69 ± 0.04 *	0.66 ± 0.06 *	0.14

Data are mean ± SD. Oxygen consumption ($\dot{V}O_2$); carbon dioxide output ($\dot{V}CO_2$); respiratory exchange ratio (RER); minute ventilation ($\dot{V}_E$); respiratory rate (f_B); tidal volume (V_T); end-tidal oxygen ($P_{ET}O_2$); end-tidal carbon dioxide ($P_{ET}CO_2$); mixed expired carbon dioxide ($PECO_2$).

*Within group, rest vs. peak exercise, $P<0.05$. Table *P*-values and symbols represent significance after Tukey-Kramer post-hoc testing from repeated measures ANOVA models.

Table 3

Alveolar equation, related derivatives, and blood biochemistry parameters

	All	HFrEF	HFpEF	*P*-value
Rest	N = 59	N = 32	N = 27	
V_D (L)	0.24 ± 0.10	0.26 ± 0.08	0.22 ± 0.13	0.64
$\dot{V}_D$ (L/min)	4.0 ± 1.7	4.3 ± 1.3	3.5 ± 2.2	0.79
V_A (L)	0.29 ± 0.11	0.28 ± 0.11	0.30 ± 0.11	0.98
$\dot{V}_A$ (L/min)	4.64 ± 1.43	4.67 ± 1.32	4.61 ± 1.57	0.99
PaO_2 (mm Hg)	71 ± 12	71 ± 14	72 ± 11	0.99
PAO_2 (mm Hg)	96 ± 7	98 ± 8	94 ± 6	0.11
PA-aO_2 (mm Hg)	25 ± 12	26 ± 13	22 ± 11	0.54
PA-$aO_2/\dot{V}O_2$ (mm Hg/mL/kg/min)	9.6 ± 5.0	10.5 ± 5.7	8.5 ± 3.8	0.41
DLO_2 (mL/min/mm Hg)	12 ± 7	12 ± 8	13 ± 7	0.98
$PACO_2$ (mm Hg)	39 ± 4	38 ± 5	40 ± 4	0.45
SaO_2 (%)	94 ± 3	94 ± 3	95 ± 3	0.88
pHa	7.41 ± 0.04	7.42 ± 0.04	7.39 ± 0.05	0.19
HCO_3^- (mEq/L)	24.33 ± 2.52	24.23 ± 2.78	24.46 ± 2.22	0.99
Base excess (mEq/L)	−0.50 ± 2.60	−0.44 ± 2.71	−0.56 ± 2.50	0.98
Peak exercise				
V_D (L)	0.38 ± 0.15 *	0.43 ± 0.15 *	0.31 ± 0.12 *	<0.01
$\dot{V}_D$ (L/min)	11.4 ± 4.8 *	12.9 ± 4.3 *	9.7 ± 4.9 *	<0.01
V_A (L)	0.71 ± 0.28 *	0.70 ± 0.26 *	0.72 ± 0.30 *	0.98
$\dot{V}_A$ (L/min)	21 ± 7 *	20 ± 6 *	21 ± 7 *	0.97
PaO_2 (mm Hg)	76 ± 15	78 ± 14 *	74 ± 15	0.59
PAO_2 (mm Hg)	109 ± 6 *	111 ± 7 *	107 ± 5 *	0.10
PA-aO_2 (mm Hg)	33 ± 14 *	33 ± 14 *	33 ± 14 *	0.99
PA-$aO_2/\dot{V}O_2$ (mm Hg/mL/kg/min)	4.3 ± 2.7 *	4.3 ± 2.6 *	4.3 ± 2.9 *	0.99
DLO_2 (mL/min/mm Hg)	29 ± 21 *	27 ± 18 *	31 ± 25 *	0.81
$PACO_2$ (mm Hg)	35 ± 6 *	34 ± 6 *	37 ± 5 *	0.03
SaO_2 (%)	95 ± 4	95 ± 3	94 ± 5	0.63
pHa	7.40 ± 0.05	7.42 ± 0.04	7.38 ± 0.05	0.02
HCO_3^- (mEq/L)	21.62 ± 3.23 *	21.19 ± 3.75 *	22.13 ± 2.47 *	0.61
Base excess (mEq/L)	−3.04 ± 3.21 *	−3.21 ± 3.62 *	−2.83 ± 2.70 *	0.96

Data are mean ± SD. Physiologic dead space (V_D); V_D ventilation ($\dot{V}_D$); alveolar volume (V_A); alveolar ventilation ($\dot{V}_A$); arterial oxygen tension (PaO_2); alveolar oxygen tension (PAO_2); alveolar-to-arterial O_2 gradient (PA-aO_2); pulmonary oxygen uptake ($\dot{V}O_2$); estimated pulmonary diffusing capacity for oxygen (DLO_2); alveolar carbon dioxide tension ($PACO_2$); arterial oxygen saturation (SaO_2); arterial pH (pHa); bicarbonate (HCO_3^-);.

*Within group, rest vs. peak exercise, $P<0.05$. Table P-values and symbols represent significance after Tukey-Kramer post-hoc testing from repeated measures ANOVA models.

Table 4

Univariate predictors of $\dot{V}_E/\dot{V}CO_2$ slope

	b (95% CL)	β (95% CL)	Intercept (95% CL)	R^2 (95% CL)	*P-value*
HFrEF					
$\dot{V}_D$	33 (8, 59)	0.44 (0.11, 0.68)	29 (18, 41)	0.20 (−0.03, 0.43)	0.01
$\dot{V}_A$	0.26 (−0.40, 0.92)	0.14 (−0.22, 0.47)	38 (24, 52)	0.02 (−0.07, 0.11)	0.43
PaO_2	0.11 (−0.18, 0.40)	0.14 (−0.22, 0.47)	35 (12, 58)	0.02 (−0.07, 0.11)	0.45
PAO_2	1.29 (0.89, 1.69)	0.77 (0.58, 0.88)	−100 (−144, −55)	0.59 (0.39, 0.79)	<0.001
PA-aO_2	0.19 (−0.10, 0.49)	0.24 (−0.12, 0.54)	37 (26, 48)	0.06 (−0.09, 0.21)	0.19
DLO_2	1.41 (−0.16, 2.99)	0.32 (−0.03, 0.60)	37 (29, 45)	0.10 (−0.08, 0.28)	0.08
$PACO_2$	−1.37 (−1.87, −0.87)	−0.72 (−0.85, −0.50)	90 (73, 107)	0.51 (0.28, 0.74)	<0.001
HCO_3^-	−1.70 (−2.64, −0.76)	−0.56 (−0.76, −0.26)	79 (59, 100)	0.31 (0.06, 0.56)	<0.01
Base excess	−1.44 (−2.48, −0.40)	−0.46 (−0.70, −0.13)	39 (34, 44)	0.21 (−0.02, 0.44)	<0.01
HFpEF					
$\dot{V}_D$	31 (8, 53)	0.49 (0.14, 0.73)	25 (17, 32)	0.24 (−0.02, 0.50)	<0.01
$\dot{V}_A$	0.00 (−0.42, 0.44)	0.01 (−0.37, 0.39)	34 (25, 44)	0.00 (0.0, 0.0)	0.98
PaO_2	−0.03 (−0.24, 0.18)	−0.06 (−0.43, 0.33)	36 (21, 52)	0.00 (−0.04, 0.04)	0.77
PAO_2	0.92 (0.38, 1.47)	0.57 (0.24, 0.78)	−65 (−124, −7)	0.33 (0.06, 0.60)	<0.01
PA-aO_2	0.13 (−0.08, 0.35)	0.25 (−0.14, 0.58)	30 (22, 37)	0.06 (−0.10, 0.22)	0.21
DLO_2	0.95 (−0.09, 1.98)	0.35 (−0.03, 0.64)	30 (25, 35)	0.13 (−0.09, 0.35)	0.07
$PACO_2$	−0.80 (−1.40, −0.20)	−0.48 (−0.73, −0.12)	64 (41, 86)	0.23 (−0.03, 0.49)	0.01
HCO_3^-	−0.40 (−1.66, 0.87)	−0.13 (−0.49, 0.26)	43 (15, 71)	0.02 (−0.08, 0.12)	0.53
Base excess	−0.04 (−1.21, 1.12)	−0.02 (−0.40, 0.36)	34 (30, 39)	0.00 (−0.01, 0.01)	0.94

Data are model parameters from univariate linear regressions predicting $\dot{V}_E/\dot{V}CO_2$ slope from rest to peak exercise in heart failure with reduced (HFrEF, N=32) or preserved (HFpEF, N=27) ejection fraction. Standardized beta (β). See definition of variables in Table 3 caption.